

OBSERVATION OF THE GEOMETRY OF COLLIDING PROTON-PROTON BEAMS BY MEANS OF BEAM-BEAM ELASTIC COLLISIONS

G. Barbiellini, M. Bozzo, P. Darriulat, G. De Zorzi, A. Fainberg, C. Grosso-Pilcher, M. Holder, A. McFarland, M. Macri, G. Maderni, S. Orito, J. Pilcher, C. Rubbia, A. Santroni, G. Sette, A. Staude, P. Strolin and K. Tittel

III. Physikalisches Institut der Technischen Hochschule, Aachen, Germany.
CERN, Geneva, Switzerland.

Department of Physics, Harvard University, Cambridge, Massachusetts 02138 (USA).

Istituto di Fisica dell'Università, INFN, Sezione di Genova, Genova, Italy.

Istituto di Fisica dell'Università, INFN, Sezione di Torino, Torino, Italy.

(presented by P. Strolin)

1. Introduction

A non-destructive observation of the geometry of coasting beams in the Proton Intersecting Storage Rings (ISR) cannot be easily performed with conventional techniques¹⁾ since i) in the absence of bunching the RF beam monitors are ineffective, and ii) the ultra-vacuum makes it almost impossible to use beam profile indicators based on ionization collection²⁾. The latter method has, in fact, led to the proposal of rather complicated techniques in which the ionization is artificially increased by scanning the coasting beams with intense molecular or atomic beams³⁾. These methods cannot be continuously applied near to the interaction points where the physics experiments are performed, since local pressure increases of several orders of magnitudes are clearly unacceptable. Furthermore, if used continuously they would perturb the geometry of the beams appreciably.

We have considered yet another possibility for continuous, non-destructive observation of the geometry of the beams, based on the reconstruction of some specific type of beam-beam collisions. In fact in the almost perfect vacuum conditions of the ISR, by far the most apparent effect of the beams is that of beam-beam interactions. Amongst the very many different types of events, elastic scatterings are ideally suited for our purposes since:

i) they occur in great abundance, i.e. $\geq 15\%$ of all interactions⁴⁾;

ii) most events give scattered particles within a narrow forward angular cone; at 24 GeV, approximately 70% of all elastic events are emitted between 6 and 26 mrad, which is the angular range of the present work;

iii) they can be promptly identified by a simple collinearity requirement in the c.m. system⁴⁾.

In order to exemplify the method, we have analysed events collected during an experiment at the ISR on small-angle elastic scattering⁴⁾. The specific application had not been envisaged at the time of the design of the apparatus. A specifically designed apparatus could be much simpler, more precise, and about one order of magnitude faster in the data acquisition rate. A very modest on-line computer could reconstruct these events for immediate display of the results.

2. The method

The principle of the method is shown in Fig. 1. The vertex of the interaction is determined by the tracks reconstructed in the wire chamber telescopes W_1 and W_2 . The analysis of a sufficiently large sample of events provides a map of the beam-beam interaction diamond, such as the one shown in Fig. 2.

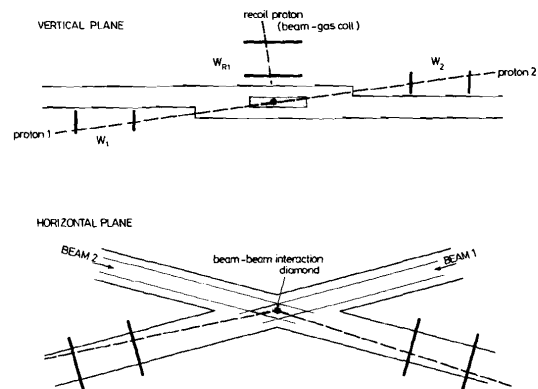


Fig. 1 : Schematic view of the experimental arrangement. The wire chamber telescopes W_1 and W_2 detect the forward scattered protons. The telescope W_{R1} detects the recoil protons scattered out in collisions with the residual H_2 in the vacuum chamber.

Histograms of the horizontal profiles of the single beams are sorted out by viewing the diamond along the respective beam directions. In a way, we are making use of one beam in order to take the horizontal scan of the other one. The resolution of each wire plane is ~ 0.35 mm. The geometry of the set-up (distance between the chambers, distance from the beam-beam diamond and from the vacuum chamber window) determines how this and some multiple Coulomb scattering on the vacuum chamber window reflect onto the resolution in the reconstruction of the vertex. In practice, a spatial resolution of a fraction of a millimetre is easily achieved, which is largely adequate when compared to the relatively large dimensions of the stored beams.

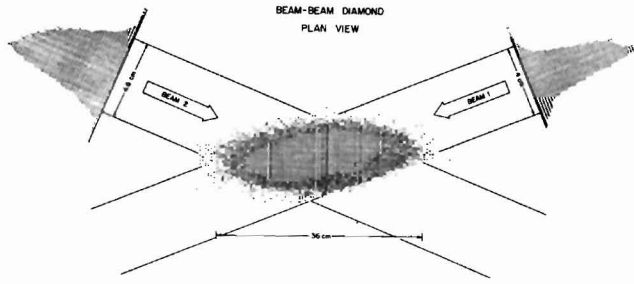


Fig. 2 : Horizontal distribution of 65,000 reconstructed vertices and horizontal profiles of the single beams.

3. The apparatus

One of the nine chamber telescopes is shown in Fig. 3. It consists of six magnetostrictive chambers accurately positioned on a rigid reference plane, which also supports the trigger counters, not shown in the figure. The chambers have been designed in order to be fully sensitive ~ 7 mm away from the vacuum chamber, so as to permit detection of small-angle scattering events with the longest possible lever arm between the chamber planes.

The beam-beam elastic event rate has been typically of the order of 300 per second at 2.5×2.5 A² circulating currents. Unfortunately, in order to prevent refiring, the present type of chambers could not be operated faster than 30 per second. This limitation could be easily overcome by using multi-wire proportional chambers.

Data acquisition and analysis is simple and fast. It has been done in the general context of the experiment, which uses an IBM 1800 on-line computer. A few thousand events give a quick test of the beam quality. High statistic beam profiles may require as many as 10^4 events.

4. Experimental observations

We present observations of typical beam evolutions during several hours of unperturbed operation of the ISR. Observations usually have extended over as many as 10^{10} revolutions. We would like to discuss some of these findings, mainly in order to elucidate the potentialities of the method.

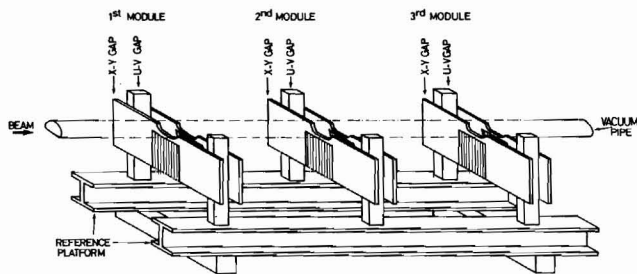


Fig. 3 : Wire spark chamber telescope.

We have divided our observations into two typical cases of "low" beam currents (~ 1.5 A \times 1.5 A) and "high" beam currents (~ 2.5 A \times 2.5 A). It is already known¹⁾ that in the case of more intense beams the beam lifetime is considerably shortened and the beam-beam effective height, which is related to the luminosity, grows up much faster. Our observations complete this picture.

Figures 4 and 5 show the observations for two-hour runs for the "low" and "high" currents conditions respectively. The time dependence of several parameters are shown in Fig. 6.

The currents circulating in the two rings are I_1 and I_2 . We indicate with $(x - x_0)$ the displacement of average beam position starting from the initial positions x_0 . The sign conventions are such that $x - x_0 < 0$ means spiralingization to a smaller radius. A first important observation is that a radial change, negligible for "low" beam currents, is clearly noticeable at "higher" currents (Fig. 6).

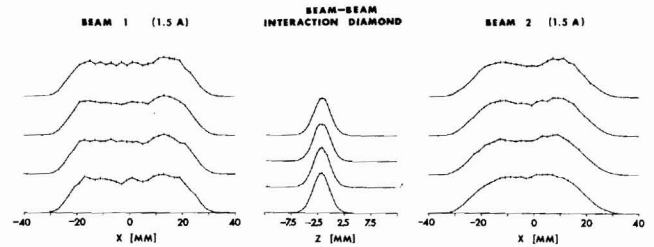


Fig. 4 : Evolution of the horizontal beam profiles and of the vertical profile of the diamond during a low-current run (x positive towards the outside of the ISR, z positive upwards).

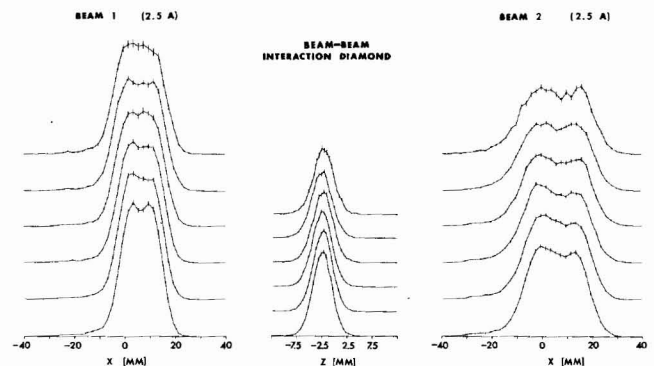


Fig. 5 : Evolution of the horizontal beam profiles and of the vertical profile of the diamond during a high-current run.

The beam 2, which presents approximately a three times as fast rate of current loss exhibits also a radial shift rate that is about twice as fast. We attribute these shifts to the presence of an additional average energy dissipation of 10^{-3} eV/turn and of 2×10^{-3} eV/turn for beams 1 and 2, respec-

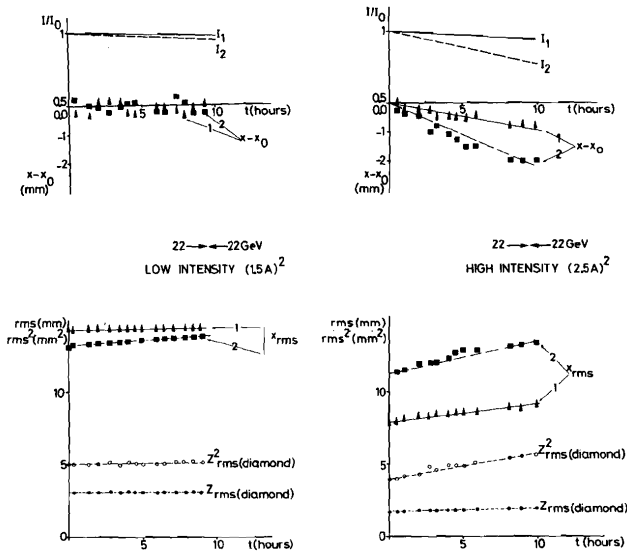


Fig. 6 : Evolution of beam parameters during low and high intensity runs.

tively. Ionization losses in the residual gas in the vacuum chamber are insufficient to account for the effect at least at the quoted average ring pressures.

Another clear effect is apparent in the increments of the squared mean deviations from the central orbit in the vertical component of the beam-beam interaction volume. Since the vertical shape of the single beams is approximately Gaussian (see Section 5), the various contributions to z_{rms}^2 add linearly. By describing $z_{rms}^2(t)$ in the form

$$z_{rms}^2(t) = z_{rms}^2(0) + At,$$

we find constant values for A, $A = 10^{-2} \text{ hour}^{-1} \text{ mm}^2$ for the "low" current condition and $A = 10^{-1} \text{ hour}^{-1} \text{ mm}^2$ for the "high" current case. The calculated multiple Coulomb scattering on the residual average gas pressures of 5×10^{-11} Torr N_2 equivalent in the two rings, although in reasonable agreement with the first case, is insufficient to explain the second anomalously large value of A. Of course one cannot exclude the possibility that indeed somewhere in the machine the residual gas pressure could have been considerably increased by the beam itself, exceeding the average values provided by the gauges.

Furthermore, we observe a substantial increment in the r.m.s. horizontal beam width x_{rms} , again much faster in the high current conditions. Moreover, if one transposes the observed vertical blow-up to the horizontal plane, one calculates values for the blow-up that are much smaller than the observations.

Finally, the aperture limitations are at all times far beyond the observed limits of the profiles of Figs. 4 and 5. Hence a simple multiple scattering causing a gradual beam blow-up and final beam losses at the limits of the acceptance cannot be the main cause of the increased current losses at higher currents.

5. Observation of vertical single beam profiles with elastic beam-gas collisions

We have demonstrated the feasibility of observing the vertical beam profile of a single beam by reconstructing, also with spark chambers, the vertex of the forward proton with the recoil proton generated by elastic scatterings of the protons of one of the beams with the residual hydrogen gas in the vacuum chamber. Because of the high quality of the vacuum which is normally provided ($\leq 10^{-11}$ Torr) in order to have an acceptable beam-gas interaction rate of the order of 10 per second, we have produced a modest temporary increase of the gas pressure by heating the vacuum chamber walls locally. The profile of a single beam and of the beam-beam are shown in Fig. 7. They are well-consistent with each other, as well as with the effective beam-height measurements using the beam displacement method^{1,5}).

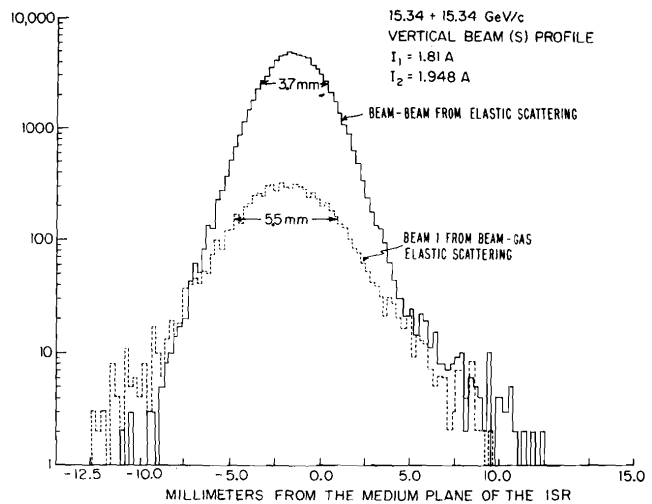


Fig. 7 : Vertical profile of a single beam and of the diamond from beam-gas and beam-beam scattering data.

Acknowledgements

We would like to express our gratitude to the ISR staff, and in particular to Drs. K. Johnsen, F. Bonaudi, E. Jones and E. Fischer for constant interest, support, and encouragement.

References

- 1) J. Borer, S. Hansen, E. Jones, M. de Jonge, B.W. Montague, D. Neet, B. de Raad, W. Schnell, L. Thorndahl, K. Unser, S. Van der Meer, H. Verelst, B. Vosicki and K. Zankel, Instrumentation and beam diagnostics in the ISR, paper presented at this conference.
- 2) C.D. Johnson and L. Thorndahl, The CPS gas ionization beam scanner, Proc. of the National Acc. Conference, Washington (1969).
- 3) B. Vosicki, Beam profile indicator, CERN internal note ISR (1968), unpublished.

- E. Kouchnirenko, P. Strolin, B. Vosicki and
K. Zankel, CERN internal report NP 70-28 (1970).
- 4) M. Holder, E. Radermacher, A. Staude,
G. Barbiellini, P. Darriulat, M. Hansroul,
S. Orito, P. Palazzi, A. Santroni, P. Strolin,
K. Tittel, J. Pilcher, C. Rubbia, G. De Zorzi,
M. Macri, G. Sette, C. Grosso-Pilcher,
A. Fainberg and G. Maderni, Phys. Letters 35 B,
355 (1971) and Phys. Letters 35 B, 361 (1961).
- M. Holder, E. Radermacher, A. Staude,
G. Barbiellini, P. Darriulat, P. Palazzi,
A. Santroni, P. Strolin, K. Tittel, J. Pilcher,
C. Rubbia, M. Bozzo, G. De Zorzi, M. Macri,
S. Orito, G. Sette, C. Grosso-Pilcher,
A. Fainberg and G. Maderni, submitted to
Physics Letters (1971).
- 5) S. Van der Meer, CERN internal report
ISR-PO/68-31 (1968).

DISCUSSION

M. Q. BARTON: Would someone from the ISR staff
comment on the slow change of radius?

W. SCHNELL: We have been aware of this effect and
at present have no explanation. When we have time,
we shall investigate it.